



9<sup>th</sup> International Conference on Photonic Technologies - LANE 2016

## Evolutionary-based design and control of geometry aims for AMD-manufacturing of Ti-6Al-4V parts

Mauritz Möller<sup>a,\*</sup>, Nicolaj Baramsky<sup>b</sup>, Ake Ewald<sup>b</sup>, Claus Emmelmann<sup>a</sup>, Josef Schlattmann<sup>b</sup>

<sup>a</sup>*Institut of Laser and System Technologies (iLAS), Hamburg University of Technology (TUHH), Am Schleusengraben. 14, 21029 Hamburg, Germany*

<sup>b</sup>*System Technologies and Engineering Design Methodology, Hamburg University of Technology (TUHH), Denickestr. 17, 21073 Hamburg, Germany*

---

### Abstract

Additive Metal Deposition (AMD) is an additive manufacturing process building parts based on a nozzle-fed powder by laser assisted solidification. The AMD technology offers unique advantages for the production of near net-shape parts. In contrast to the powder bed-based technologies it provides a high productivity grade.

Today AMD lacks reproducible process strategies manufacturing large parts in narrow tolerances. The building height of a single layer and the geometrical shape of a whole part alter progressively with increasing part dimensions - consecutively leading to a higher effort in the manufacturing-process development for such parts.

To reduce this effort, in this paper first an iterative identification of optimal process parameters is performed by following an evolutionary algorithm under varied BC. Based on the geometry-related parameter sets, tolerances are defined. The process strategies and tolerances are validated for a prototype application considering the defined quality aims. Finally the results are discussed and summarized in an a-priori process design guideline for AMD Ti6Al4V-parts.

© 2016 The Authors. Published by Elsevier B.V. This is an open access article under the CC BY-NC-ND license

(<http://creativecommons.org/licenses/by-nc-nd/4.0/>).

Peer-review under responsibility of the Bayerisches Laserzentrum GmbH

*Keywords:* additive manufacturing; titanium; design guideline; evolutionary algorithms

---

---

\* Corresponding author. Tel.: +49-176-1484-0130 .  
E-mail address: [mauritz.moeller@lzn-hamburg.de](mailto:mauritz.moeller@lzn-hamburg.de)

## 1. Introduction

Nowadays Titanium parts are widely used in aerospace applications due to the excellent specific mechanical properties. The need for lightweight design in aerospace industries leads to expensive production due to subtractive manufacturing resulting in mass reduction of the raw material of up to 95%. The Additive Metal Deposition (AMD) is a layer-by-layer manufacturing process for the production of three-dimensional complex parts (Ravi et al. 2013). The repair of high value parts using AMD were shown by Brandl 2010 and Thijs et al. 2010. The additive manufacturing process offers a high geometrical flexibility in comparison to conventional manufacturing technologies like Laser Additive Manufacturing (LAM) (Brandl 2010).

The successful application of AMD requires on the one hand stable process parameter sets to build three-dimensional parts with a reproducible quality as well as design guidelines to record freedom and restriction of the manufacturing process.

Process parameters can be developed using biasless tools like evolutionary algorithms, where a fast identification of ideal process parameters is possible. According with an increasing height of AMD parts the material properties are altering progressively (Paydas et al. 2015). Therefore process strategies are needed, that support the variation of parameters relative to the height of the product, due to the changing thermal boundary conditions with increasing height. Design guidelines have been published for related additive manufacturing processes like LAM by Kranz et al. 2015 and Adam 2015 during recent years, that show the restrictions of these manufacturing processes. Named guidelines cannot be fully applied on AMD, because, different to LAM, in AMD there is no interaction, like structural support and thermal conductivity during the manufacturing process, between the powder and the product.

Previous publications by Paydas et al. 2015, Kelbassa 2006 and Brandl 2010 on the AMD process have investigated the mechanical properties of the layer-by-layer added material. In addition, Paydas et al. 2015 studied the influence of the welding path on the microstructure and Fessler et al. 1996 investigated the residual stresses in built up AMD products. These publications show the usability of AMD manufactured parts as structural components.

Guidelines by Kranz et al. 2015 were developed to be able to exploit the full geometrical and lightweight design potential of LAM processes. Basic shapes in lightweight design can be extracted from guidelines for general lightweight design (Klein 2009). Design methods in lightweight design often cause fine structured parts, which are mostly a result of mass optimization (Wiedemann 2007). Basic shapes introduced by Wiedemann 2007 are thin walls, beam elements, rib elements and hollow structures.

## 2. Method and set-up

The investigations are executed with a TrumpfTruDisk 6001 multi-mode continuous wave disk laser with a laser power of 6 kW at a wavelength of 1.03  $\mu\text{m}$ . A three nozzle processing head is used with an rotational table feeder (Fig. 1). To ensure an inert atmosphere, argon is used in a shielding cabin with measured less than 50 ppm of residual oxygen. The used Ti-6Al-4V powder is spherical and sieved to fraction of 45 to 90  $\mu\text{m}$ .

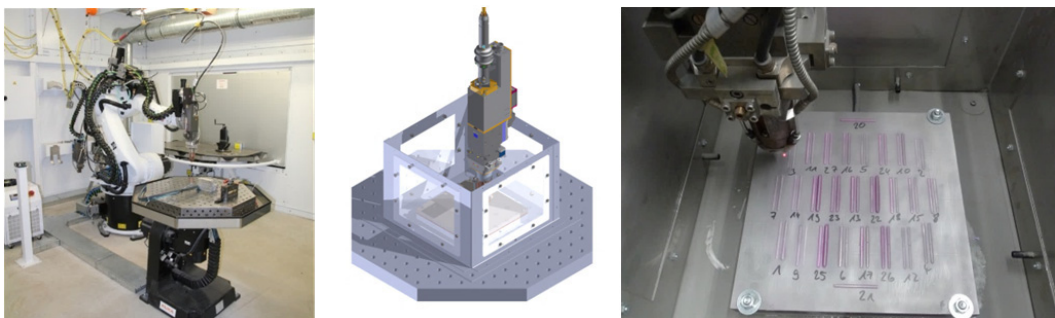


Fig. 1. (a) robot cell (TruLaserRobot); (b) shielding cabin for argon atmosphere; (c) processing head applying single bead welds on base plate in the shielding cabin.

### 3. Evolutionary-based development of stable

#### 3.1. Algorithm and Constraints

The process of laser cladding depends on a number of parameters heavily interfering with each other. The solution space is very large and exhaustive search of the optimum becomes impractical. Partly objectives are conflicting, e.g. a high cladding rate and a high surface quality, and the time to achieve one solution (test run on the machine) takes long. Guessing of parameter sets for a design of experiments could lead to a high number of test runs due to unintentional mistakes. To compensate this the use of evolutionary algorithms is common in real world applications (Chiong 2012). We decided for an algorithmic approach using the multi-objective genetic algorithm (GA) NSGA-II Deb (2000, 2002). This allows us to address a number of dependent objectives at a time and to find the pareto front, which enables us to weight the objectives afterwards and choose parameter sets for different requirements in the cladding process. A GA uses recombination and mutation of the best results of the past iteration to determine the parameters for the next generation thus progressively improving the pareto front in all defined dimensions. The NSGA-II algorithm is well studied, broadly used, and since the number of objectives is relatively small, the algorithm ensures a good performance for this task (Coello 2007).

The investigated parameters are the laser power [W], the velocity [m/s] of the nozzle, and the feeding rate of the powder [U/min] (angular velocity of the feeder). The objectives are the height of the wall [mm], the optical appearance [1: good to 10:bad], and the rate of cracks [1: good to 10:bad].

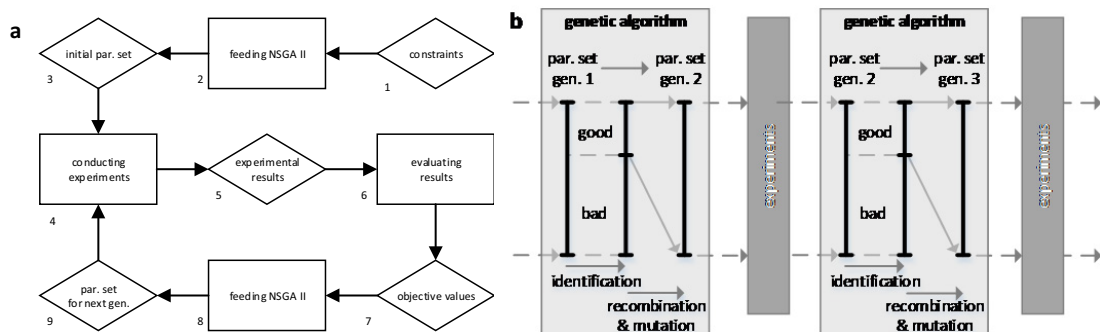


Fig. 2. (a) structure chart, (b) working principle of the genetic algorithm.

The GA demands for a minimization which is taken care of in the programming. To increase the effectiveness, the NSGA-II was modified to work with integer values for the parameters only. That allows us to precisely control the variable space with discrete values and reduces the total number of possible parameter combinations.

Fig. 2 (a) shows the procedure that was used to conduct the experiments in collaboration with the GA. The initial parameter set was determined (2) by the algorithm after all constraints for the parameters had been defined (1). These were used to run the tests for the first generation (4). The samples were analyzed (5) and the points for the achievement of the defined goals were evaluated (6). Feeding back the obtained values into the algorithm (8) results in the next set of parameters for the next generation (9).

Before starting the next generation, the parameter set was investigated. Due to the operating principles of the algorithm, the possibility to generate a parameter set which has already been tested is greater than zero. These duplicates were replaced with more meaningful values to maximize the available machine time by restarting the algorithm which yields different results each time due to some randomized steps in the algorithm. The parameters were chosen to be close to parameters sets of good quality. In order to do so, processing speed and powder feed rate were slightly increased. The bandwidth of the process parameters is illustrated in table 1. These parameters describe the optimization space used by the evolutionary algorithm to identify an optimized parameter set.).

Table 1. Process parameter set for evolutionary algorithm.

| Laser power [W]  | Processing speed [m/s] | Feeder rotation [U/min] |
|------------------|------------------------|-------------------------|
| 1.000 – 2.000    | 0,5 – 1,2              | 4 – 10                  |
| increment: 100 W | increment: 0,1 m/s     | increment: 1 U/min      |

The feeder rotation rate is linked to the mass of fed particle mass. The correlation between the feeder rotation rate and the particle mass for is measured and illustrated in figure 3.

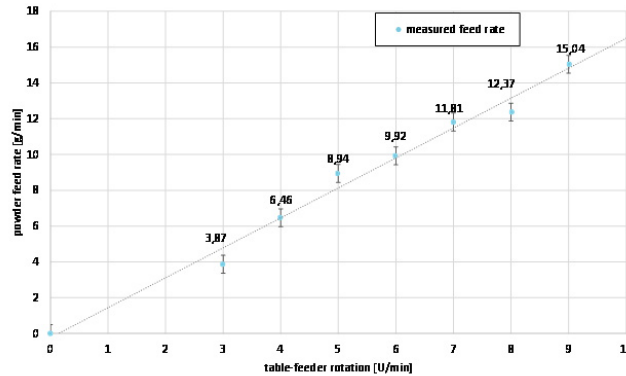


Fig. 3. Measured dependency between table-feeder rotation and powder feed rate (carrier gas: 5 l/min).

### 3.2. Results

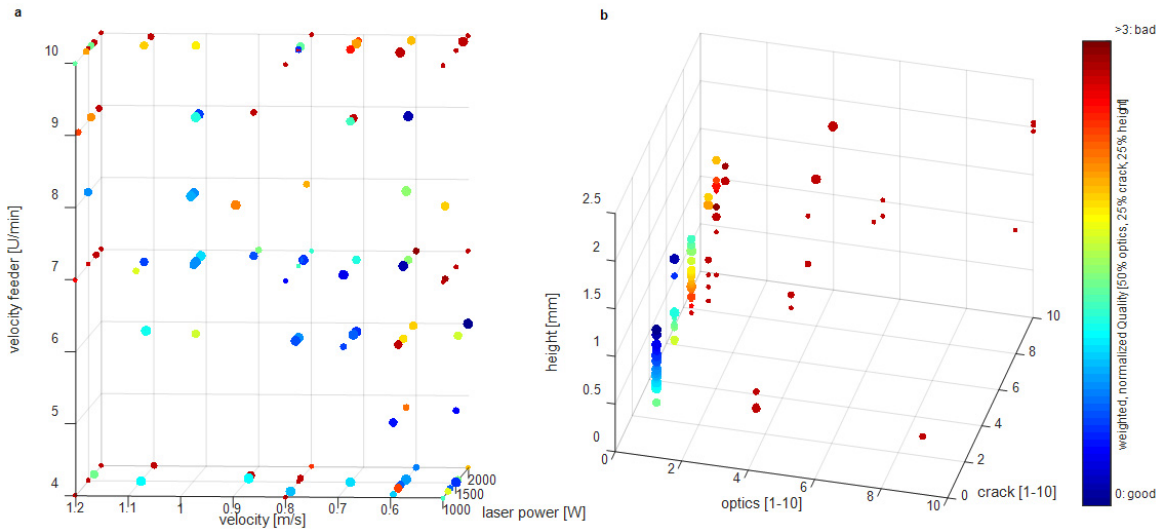


Fig. 4. (a) test parameters and (b) results of batch 1 with weighted, normalized quality. Circle size denotes the generation (smallest to largest).

For the first run with three variables and three objectives with a total number of  $11 \cdot 8 \cdot 7 = 616$  possible combinations 108 (17.5%) individual tests within four generations with a population of 28 tests have been conducted. Over the four generations a significant improvement of the parameter sets can be seen. The variable space is depicted in Fig. 4. (a), the solution space in Fig. 4. (b). The color of the circles shows the weighted and

normalized quality ranging from 1 to 10 point with 1 being the best. The size of the circles shows the generation with the largest being the latest generation. The parameter are well distributed in the variable space.

In the center part of Fig. 4. (a) an area with good results (blue) can be seen. The boundaries of the defined variable space seems to produce less good results which confirms the choice for the boundary values. However, there are some individual very good results (dark blue) spread throughout the variable space. That either shows the complex dependency between the parameters or there exist factors that we have not considered in this approach. The solution space, Fig 4. (b) shows a strong development over the generations towards good results. Singular bad results (big red circles) are an effect of the GA. At the last generation, the majority of the samples delivered very good optical values. An increase in height mostly resulted in bad crack values.

### 3.3. Development of threedimensional process strategy

Fig. 5 shows the four evolutions where each row represents a single evolution. The evolutionary algorithm is used for the development of two-dimensional process parameters for single beads (Fig. 4). The increasing amount of good results (green marker) shows the value of the evolutionary algorithm in finding the optimized parameter set. After developing two-dimensional parameter sets the strategy for three-dimensional building of parts in narrow tolerances has to be considered.

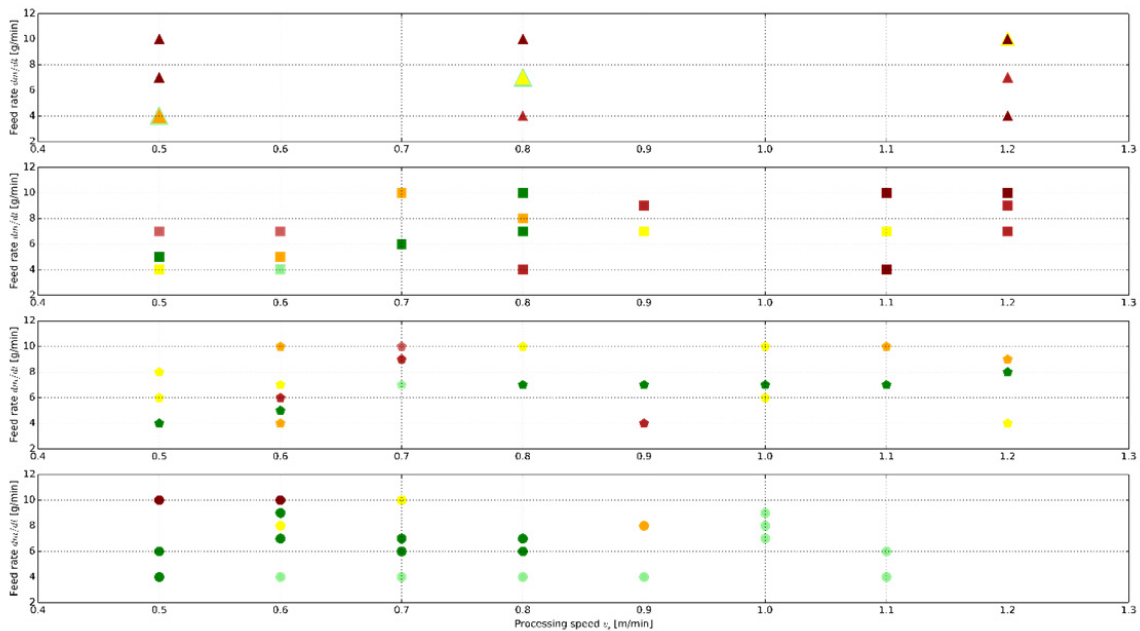


Fig. 5. Quality of the manufactured single beads (red: low quality ; green: high quality).

For a first approach the most efficient set of parameters is chosen to manufacture a wall without any optimization (laser power: 1.500 W; processing speed: 0,6 m/min; table rotation: 7 U/min). The dimensions for the wall are described in figure 6 (a). The produced wall shows high accuracy in height ( $68,03 \text{ mm} \pm 0,089$  (standard deviation)). But it also reveals an irregular wall thickness in the micrograph in figure 6 (b) ( $4,65 \text{ mm} \pm 0,40$  (standard deviation)). The irregular shape leads to a higher effort in post processing like additional milling processes. The aim is to achieve a predictable shape with less need for final machining to ensure the desired dimensions of the part. To do so there are three phases identified in the micrograph (Fig. 7 (c)). The first phase shows an increasing thickness of the wall. This can be explained by the high initial need of energy caused by the heat capacity of the base plate on the one hand and the threedimensional heat conduction in the base plate on the other hand (extend to approx. 5 mm

in height). With increasing build height the process approximately comes to an equilibrium state in the second phase with an approximated two-dimensional heatflow (extend to approx. 38 mm in height). The third phase shows an decreasing thickness related to the upcoming heat accumulation.

To deal with the varying thermal situation in tree-dimensional parts, one approach is to implement sensors in order to control the parameters for the changed boundary conditions. The approach in this paper is about designing a robust process, which can be defined a-priori and doesn't need on-line adjustments. Therefore the main influencing

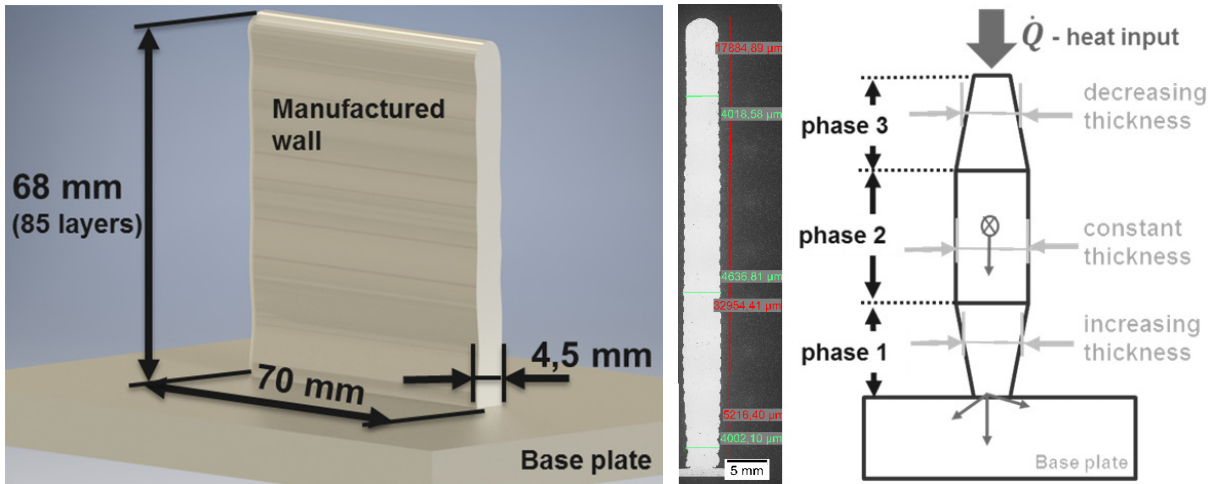


Fig. 6. (a) Specimen dimensions; (b) Micrograph of wall w/o optimization; (c) Empirical model of wall thicknesses in three phases.

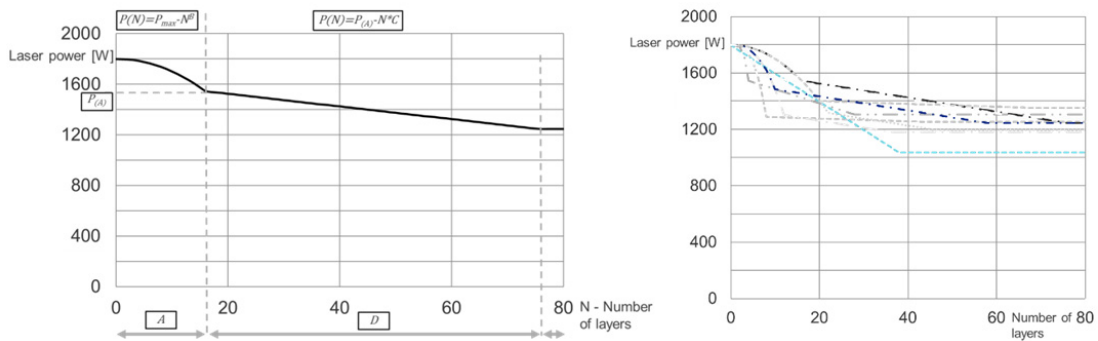


Fig. 7. (a) Process strategy for threedimensional approximate isothermal build strategies; (b) Laser power development for the nine examined process strategies.

quantity, the heat input, is defined variable with the build height. Based on this a basic heat input model is introduced. To get an approximately isothermal process, the laser power is chosen to vary the heat input.

The four variables A, B, C and D are varied to compare different threedimensional process strategies (Tab. 2).

Table 2. Variation of variables for empirical examination.

| A [-]        | B [-]          | C [-]        | D [-]         |
|--------------|----------------|--------------|---------------|
| 2 - 22       | 2 - 5,5        | 1 - 20       | 24 - 60       |
| increment: 2 | increment: 0,5 | increment: 5 | increment: 12 |

The goal behind the usage of a higher polynomial function in the first phase, is to reduce the laser power faster after a short and intensive heating time extending only over a few layers. The further decrease of the laser power is proportional to the number of layers.

### 3.4. Results and discussion

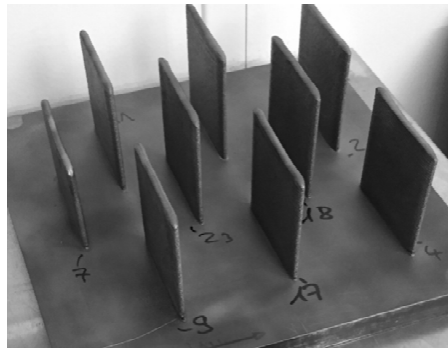


Fig. 8. Built walls with varied decrease function of heat input with progressive build height.

Outer dimensions of the built walls (Fig. 8) are measured using a CMM (Wenzel LH87) with an accuracy of  $(1,8 + L/350) \mu\text{m}$ .

Table 3. Accuracy of varied process strategies.

| Process strategy     | variable values        | height                  | width                  |
|----------------------|------------------------|-------------------------|------------------------|
| Constant laser power | -                      | 68,03 mm $\pm$ 0,089 mm | 4,65 mm $\pm$ 0,400 mm |
| 1 (2)                | A 4; B 4; C 10; D 24   | 66,74 mm $\pm$ 0,453 mm | 4,29 mm $\pm$ 0,086 mm |
| 2 (4)                | A 8; B 3; C 1; D 36    | 65,06 mm $\pm$ 0,655 mm | 4,24 mm $\pm$ 0,106 mm |
| 3 (5)                | A 12; B 2,5; C 5; D 24 | 67,46 mm $\pm$ 0,363 mm | 4,43 mm $\pm$ 0,114 mm |
| 4 (7) failed         | A 16; B 2; C 5; D 60   | 52,92 mm $\pm$ 2,333 mm | 4,14 mm $\pm$ 0,142 mm |
| 5 (9)                | A 20; B 2; C 1; D 48   | 66,71 mm $\pm$ 0,235 mm | 4,54 mm $\pm$ 0,216 mm |
| 6 (11)               | A 2; B 5,5; C 20; D 36 | 67,15 mm $\pm$ 0,486 mm | 4,45 mm $\pm$ 0,226 mm |
| 7 (17)               | A 22; B 2; C 10; D 24  | 64,85 mm $\pm$ 0,788 mm | 4,37 mm $\pm$ 0,183 mm |
| 8 (18)               | A 10; B 2,5; C 5; D 48 | 67,09 mm $\pm$ 0,357 mm | 4,36 mm $\pm$ 0,178 mm |
| 9 (23)               | A 6; B 3; C 5; D 60    | 67,23 mm $\pm$ 0,233 mm | 4,56 mm $\pm$ 0,145 mm |

The irregularity of the wall's geometry can be reduced significantly as shown in table 3. Although there is a decrease in height of the walls detected, the width accuracy of the sides has increased. Due to the fact, that the amount of post processing is mainly influenced by the sides of the walls, it is advised to optimize the AMD process for uniform wall thickness, instead of maximum height accuracy.

## 4. Preliminary guideline

### 4.1. Experiments

The following experiments show a first introduction to determine the degree of freedom using the introduced AMD system for the process in view of a design guideline. Thin walls have been selected as basic shape for the experiments. The walls have been manufactured with a length of 50mm and a width of a single lane. The specimens have been manufactured under different angles from 0 degree to 30 degree to the normal of the surface of the building platform. There are three strategies to implement the varying angles, sketched in figure 9.

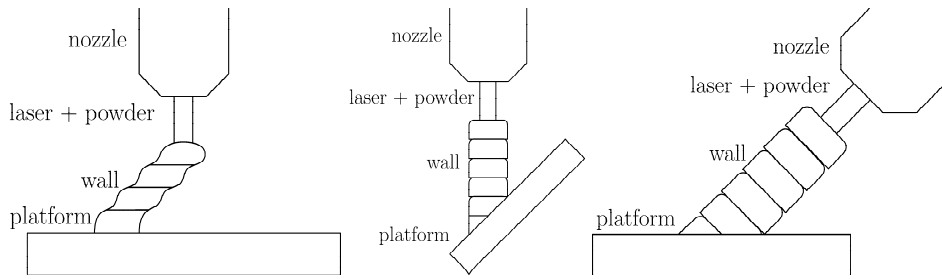


Fig. 9. Sketch of the three building strategies; left: strategy 1, middle: strategy 2 and right: strategy 3.

The first strategy realized the angle with a stepwise offset between the layer similar to the LAM process. The second strategy used the possibility of the system to vary the angle of the platform with the advantage that the process could build up the wall in direction of the gravity. The third strategy built up the wall while tilting the nozzle in direction of the building direction.

The evaluation of the surface roughness has been recorded with a Keyence VK-8710 Laser Scanning Microscope according to ISO 4287:1997. The wall thickness has been evaluated with a Series 102 micrometer (Mitutoyo) with a measurement range from 0 to 25 mm, a 0.01 mm scale and  $\pm 2 \mu\text{m}$  accuracy.

#### 4.2. Discussion

In the first step the complete built-up of the manufactured walls has been evaluated. As an example the walls of the build strategy 3 are shown in figure 10 (a). In the second step the thickness  $b$  of the built-up walls were measured just as the surface roughness  $R_a$  and  $R_z$ . Both measurements have been repeated three times per wall, one in the first third, one in the middle part and one in the last third along the 50mm length. The microscope is tracking a defined area of the surface where in the next step the roughness measuring line is positioned, exemplary shown in figure 10

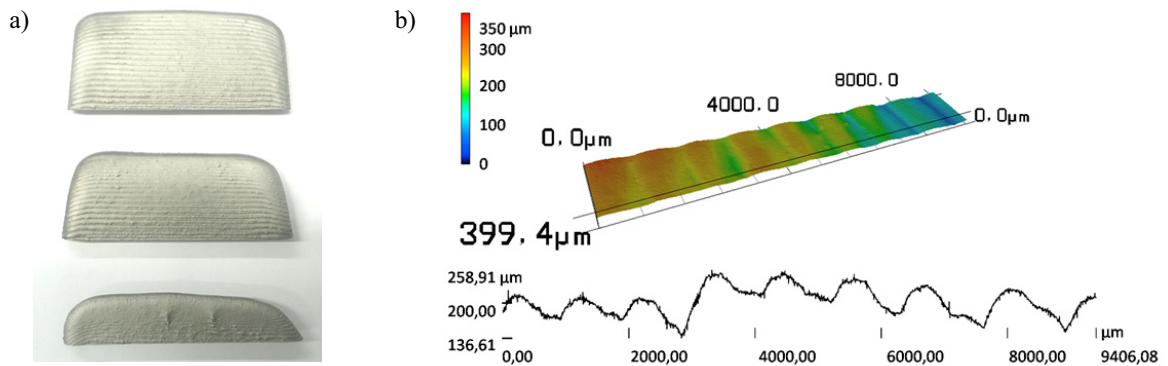


Fig. 10. (a) wall build with strategy 3, upper wall under an angle of  $10^\circ$ , middle wall  $20^\circ$  and lower wall  $30^\circ$  (b) roughness measurement, upper part show scanned 3d plane, lower part show measured roughness line.

Table 4. Matrix of all measured average values for the manufactured walls.

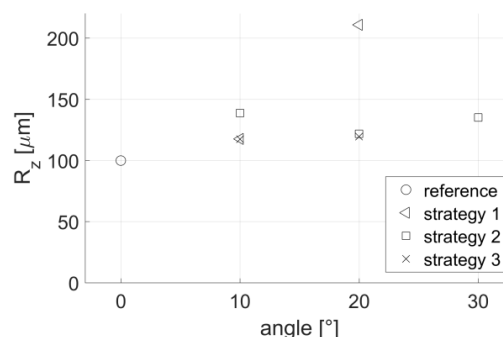
| inclination angle | Reference  | Strategy 1  | Strategy 2  | Strategy 3  |
|-------------------|--|---|---|---|
| 0°                | b=4,89 mm<br>R <sub>a</sub> =21,20 μm,<br>R <sub>z</sub> =99,79 μm |   |   |   |
| 10°               |  | b=4,49 mm<br>R <sub>a</sub> =22,66 μm,<br>R <sub>z</sub> =117,43 μm | b=4,86 mm<br>R <sub>a</sub> =28,30 μm,<br>R <sub>z</sub> =138,69 μm | b=4,68 mm<br>R <sub>a</sub> =27,11 μm,<br>R <sub>z</sub> =117,31 μm |
| 20°               |  | b=4,35 mm<br>R <sub>a</sub> =39,80 μm,<br>R <sub>z</sub> =210,87 μm | b=4,92 mm<br>R <sub>a</sub> =23,61 μm,<br>R <sub>z</sub> =121,70 μm | b=4,66 mm<br>R <sub>a</sub> =21,79 μm,<br>R <sub>z</sub> =119,49 μm |
| 30°               |  | failed  | b=4,72 mm<br>R <sub>a</sub> =29,08 μm,<br>R <sub>z</sub> =135,04 μm | failed  |

The experiments show that the different building strategies lead to different results. Strategy 1 and strategy 3 lead to failed walls at an angle of 30 degree. Strategy 3 also failed at a 30 degree angle. In contrast to the first strategy the nozzle built up the wall in direction of the wall leading to a different failure reason: The melted part of the wall bends towards the gravity. This bending affects the failure, the investigation of alternative welding parameters that reduce the bending effect could be a future objective. Strategy 2 shows the best results. The advantage of the strategy is that the built-up is along the gravity reducing most of the influences. Critical is the connection of the first layers to the platform because of the larger laser spot area by reason of the tilted platform. Up to an angle of 30 degree the connection has not been a problem.

The wall thickness *b*, illustrated in table 4, of strategy 2 is comparable to the reference wall. Strategy 3 produces walls of constant thickness but about 0,2 mm smaller than the reference wall. The highest difference of the wall thickness in comparison to the reference wall has been evaluated in strategy 1. The realisation of complex parts can be supported by building strategies that build up segments with a constant thickness. Therefore strategy 2 or alternatively 3 are recommend considering the wall thickness.

The surface quality has an influence on the optical look, the buy-to-fly-ratio and the fatigue strength. The optical look is important if a part is visible for the customer. A rough surface can create the impression of a bad quality. The fatigue strength can also be influenced by a rough surface where the surface acts as a notch and introduces cracks. To prevent the notch effect a final machining can be necessary. Also a final machining of functional planes can be necessary if the surface quality is not sufficient.

The surface roughness of the manufactured walls has been evaluated using the introduced Laser Scanning Microscope. Figure 11 shows the surface roughness as a function of the tilt angle of the wall. The results of strategy 1 show a significant rise of the surface roughness with an increasing tilt angle. Strategy 2 and 3 show a nearly constant surface roughness comparable to the reference wall. Both strategies are applicable to generate parts with a predictable surface roughness. A predictable constant surface roughness allows a valuation of the fatigue strength.

Fig. 11. Figure of R<sub>z</sub> -values of the building strategies as a function of the tilt angle of the wall.

## 5. Conclusions

The AMD process can be used to build up walls in narrow tolerances using three-dimensional adapted process strategies. This paper gives an approach to set a-priori parameters for effective dereduction of the deviation between the actual and the required dimension based on this the amount of the bandwidth can now be examined and even minimized in further research.

The AMD process as well can be used to build up thin walls under an angle up to 30 degree to the surface of the building platform.

Different building strategies have been analysed. Two out of three evaluated building strategies provide comparable measurements to the reference wall. Both strategies appear to be applicable under the identified operation conditions. Further experiments are reasonable to expand the operation conditions of the building strategies.

Besides the expansion of the building strategies for thin walls, other building strategies for other specified basic shapes have to be investigated.

## References

- Adam, Guido A. O., 2015. Systematische Erarbeitung von Konstruktionsregeln für die additiven Fertigungsverfahren Lasersintern, Laserschmelzen und Fused Deposition Modeling. Forschungsberichte des Direct Manufacturing Research Centers, Band 1. Shaker, Aachen.
- Brandl, E., 2010. Microstructural and mechanical properties of additive manufactured titanium (Ti-6Al-4V) using wire. Aachen, Shaker.
- Coello, Carlos Coello, Gary B. Lamont, and David A. Van Veldhuizen. Evolutionary algorithms for solving multi-objective problems. Springer Science & Business Media, 2007.
- Chiong, Raymond, and Thomas Weise. Variants of evolutionary algorithms for real-world applications. New York, NY, USA: Springer, 2012.
- Deb, Kalyanmoy, Amrit Pratap, Sameer Agarwal, and T. Meyarivan. A Fast and Elitist Multiobjective Genetic Algorithm: NSGA-II. IEEE Transactions on Evolutionary Computation, 6(2):182–197, April 2002.
- Deb, Kalyanmoy, et al. "A fast elitist non-dominated sorting genetic algorithm for multi-objective optimization: NSGA-II." Parallel problems solving from nature PPSN VI. Springer Berlin Heidelberg, 2000.
- Fessler, J. R., Merz, R., Nickel, A. H., Prinz, F. B., & Weiss, L. E., 1996. Laser deposition of metals for shape deposition manufacturing. In: Proceedings of the solid freeform fabrication symposium (pp. 117-124). Austin, TX: University of Texas at Austin.
- Kelbassa, I., 2006. Qualifizieren des Laserstrahl-Auftragschweißens von BLISKS aus Nickel- und Titanbasislegierungen. Fakultät für Maschinenwesen. Publikationsserver der RWTH Aachen University, Aachen.
- Klein, Bernd, 2009. Leichtbau-Konstruktion: Berechnungsgrundlagen und Gestaltung ; mit Tabellen. 8., überarb. und erw. Aufl. Vieweg + Teubner, Wiesbaden.
- Kranz, J.; Herzog, D.; Emmelmann, C., 2015. Design guidelines for laser additive manufacturing of lightweight structures in TiAl6V4. In: J. Laser Appl. (Journal of Laser Applications) 27, S14001.
- Lore Thijs, Frederik Verhaeghe, Tom Craeghs, Jan Van Humbeeck, Jean-Pierre Kruth, A study of the microstructural evolution during selective laser melting of Ti-6Al-4V, Acta Materialia, Volume 58, Issue 9, May 2010, Pages 3303-3312, ISSN 1359-6454, <http://dx.doi.org/10.1016/j.actamat.2010.02.004>.
- H. Paydas, A. Mertens, R. Carrus, J. Lecomte-Beckers, J. Tchoufang Tchuidjang, Laser cladding as repair technology for Ti-6Al-4V alloy: Influence of building strategy on microstructure and hardness, Materials & Design, Volume 85, 15 November 2015, Pages 497-510, ISSN 0264-1275, <http://dx.doi.org/10.1016/j.matdes.2015.07.035>.
- G.A. Ravi, X.J. Hao, N. Wain, X. Wu, M.M. Attallah, Direct laser fabrication of three dimensional components using SC420 stainless steel, Materials & Design, Volume 47, May 2013, Pages 731-736, ISSN 0261-3069, <http://dx.doi.org/10.1016/j.matdes.2012.12.062>.
- Wiedemann, Johannes, 2007. Leichtbau: Elemente und Konstruktion. 3. Aufl. Springer-Verlag Berlin Heidelberg. ISBN: 3540336575.